Diamond & Related Materials 18 (2009) 768–771

Contents lists available at ScienceDirect

Diamond & Related Materials

journal homepage: www.elsevier.com/locate/diamond

Characterization of EUV induced carbon films using laser-generated surface acoustic waves

Juequan Chen [a,*], Chris J. Lee [a], Eric Louis [a], Fred Bijkerk [a], Reinhard Kunze [b], Hagen Schmidt [b], Dieter Schneider [c], Roel Moors [d]

[a] FOM-Institute for Plasma Physics Rijnhuizen, Edisonbaan 14, 3439 MN, Nieuwegein, The Netherlands
[b] Leibniz Institute for Solid State and Materials Research, Helmholtzstr. 20, D-01171 Dresden, Germany
[c] Fraunhofer-Institutes for Material and Beam Technology, Winterbergstrasse 28, D-01277 Dresden, Germany
[d] ASML, Veldhoven, The Netherlands

ARTICLE INFO

Available online 3 December 2008

Keywords:
Amorphous hydrogenated carbon
EUV radiation
Surface acoustic waves
Mechanical properties

ABSTRACT

The deposition of carbon layers on the surfaces of optics exposed to extreme ultraviolet (EUV) radiation has been observed in EUV lithography. It has become of critical importance to detect the presence of the carbon layer in the order of nanometer thickness due to carbon's extremely strong absorption of EUV radiation. Furthermore, the development of efficient cleaning strategies requires that the nature of these carbon layers is well understood. Here, we present experimental results on the detection and characterization of carbon layers, grown on Mo/Si EUV reflecting optics, by laser-generated surface acoustic waves (LG-SAW). It was found that SAW pulses with a frequency bandwidth of more than 220 MHz can be generated and detected for multilayer mirrors and LG-SAW is sensitive enough to detect EUV induced carbon layers less than 5 nm thick. It was inferred from the low Young's modulus (<100 GPa) that the carbon layer induced by EUV illumination in these vacuum conditions is mechanically soft and polymeric in nature with a high percentage of hydrogen.
© 2008 Elsevier B.V. All rights reserved.

1. Introduction

Extreme ultraviolet lithography (EUVL) is a next-generation lithography technology using radiation at 13.5 nm. Contamination of optics is a critical concern in the field of EUVL because it can reduce the reflectance of Mo/Si multilayer mirrors (MLMs) for optics [1] and, consequently, the throughput of the total optical system. Thus, it is necessary to be able to either prevent the deposition of contaminating films or to nondestructively clean optics periodically. In both cases, it is necessary to understand how the contamination is deposited and the resulting layer's property. In addition, efficient cleaning requires that the presence of the contamination layer be detected early in its formation, preferably before a single monolayer is complete. Here, we use surface acoustic waves (SAW) to investigate the mechanical properties of carbon films that were grown under EUV illumination.

In a previous work, X-ray photoelectron spectroscopy (XPS) and Auger electron spectroscopy (AES) have been employed to measure the thickness of EUV induced carbon contamination films [2,3]. XPS and AES are very sensitive to the presence of carbon, but are insensitive to hydrogen, which means it cannot distinguish between a thin diamond-like film and a thick polymer-like film.

Ellipsometry has also been employed to characterize thin carbon films, though not grown on MLM [4]. The structure of the MLM is a complicating factor in characterizing surface films, however, the optical properties of the various phases of carbon films presents a larger problem. Although graphite-like films can be distinguished by their strong (sp^2) absorption in the visible-near IR region, the optical properties of sp3 dominated polymeric films are very similar to diamond-like films. Since ellipsometry only provides the optical thickness directly, one must already know the thickness and the density to obtain the phase of the carbon film. This level of *a priori* knowledge is not usually available for novel films, such as EUV induced carbon.

On the other hand, SAW have been found to be very sensitive to the characteristics of surface films, e.g. film growth even when the thickness of the layer is much smaller than the SAW wavelength [5]. The propagation of SAW depends on the acoustic properties, such as Young's modulus, Poisson ratio, density and thickness of the surface layer and the substrate, respectively. In the case of carbon, Young's modulus varies from <100 GPa for a hydrogenated, amorphous polymeric film to ~1000 GPa for a crystalline diamond film, making it highly sensitive to the phase of the carbon layer [6]. Most importantly, it is highly sensitive to the presence of hydrogen in sp^3-dominated films, thus providing a clearly sensitive method for distinguishing diamond-like and hydrogenated amorphous polymeric films.

Laser-generated SAW (LG-SAW) is a convenient and efficient method to characterize the mechanical properties of thin films because it provides a broadband acoustic pulse that, after analysis,

* Corresponding author.
E-mail address: J.Chen@rijnhuizen.nl (J. Chen).

0925-9635/$ – see front matter © 2008 Elsevier B.V. All rights reserved.
doi:10.1016/j.diamond.2008.11.030

reveals much more information than a single frequency SAW[7]. LG-SAW has been broadly used to characterize amorphous carbon films (see, e.g., [5] and references therein). However, to our knowledge, LG-SAW has never been used to investigate carbon layers grown under EUV illumination. In this paper, we present results on the mechanical properties of carbon contamination films, grown under EUV illumination (which we refer to as "EUV induced carbon"). In addition, our results show that LG-SAW measurements are robust even when the substrate has a strongly heterogeneous coating, as is the case for MLMs.

2. Experimental setup

2.1. Carbon layer deposition

Briefly, the MLMs investigated here consist of a capping layer plus 50 bi-layers of Mo and Si, each about 7 nm thick, deposited on the (001) surface of a Si wafer. The thickness of the full multilayer stack is 357 nm. A complete description of a typical MLM structure and its properties can be found elsewhere [8].

Two MLM samples were exposed to EUV radiation from a xenon-based EUV hollow cathode discharge plasma source [9]. The source emits pulses with a pulse duration of 50–100 ns at a repetition frequency of 270 Hz. The radiation in the 10–18 nm range was selected from the broadband emission by passing the light through a zirconium filter, attached to a stainless steel box. The samples were placed in the box to protect them from direct exposure to the discharge products. In addition, each mirror stack was masked so that only half the surface was illuminated, but no measures were taken to prevent hydrocarbons from diffusing under the mask and adsorbing to the surface. The distance between the source and mirror was about 50 cm. Each mirror was evenly illuminated by the filtered EUV light at an energy density of 1.9 $\mu J/cm^2$ per pulse, which is sufficiently low to prevent the mirror from heating significantly over the entire exposure time. The mirrors were exposed to 2 million (~2 hour exposure time) and 5 million (~5 hour exposure time) pulses respectively to obtain two different carbon layer thicknesses.

The residual hydrocarbon gases in the chamber act as the source for the carbon layer deposition. The vacuum in the chamber was between 10^{-6} and 10^{-7} mbar, which increased to 10^{-3} mbar while the EUV source was operating, however, this increase is entirely due to additional xenon and the partial pressure of the out-gassed hydrocarbons is not expected to vary during deposition. From the residual gas analyzer (RGA) spectrum, a hydrocarbon peak can be easily discriminated from the background. The RGA spectrum showed masses between 62 and 70 mass numbers, which corresponds to hydrocarbons around the size of pentane or larger and Xe^{2+}.

For the purposes of comparison, a second pair of MLMs had a graphitic layer deposited on their surfaces by evaporating a graphite filament in close proximity to the MLM surface in a vacuum (which we refer to as "hot filament carbon"). The graphite wire was evaporated using a current pulse. The current pulse and resulting evaporation time was estimated to less than one second. The MLM sample was placed on a copper mount, facing the wire at a distance of 5–10 cm. The short duration of the current pulse and the copper mount ensure the temperature of the mirror does not change significantly over the duration of the exposure.

A variable angle spectroscopic ellipsometer (Woollam, VASE) was used to determine the thickness of the carbon films, assuming various carbon morphologies. The films were investigated in the wavelength range from 280 to 1550 nm, and at incidence angles of 65°, 70° and 75°. The hot filament carbon layer thicknesses were determined to be 11.9 and 24.3 nm, using a Tanguy model [10]. However, the EUV induced carbon fit two models equally well, the Tauc–Lorentz [11] and Cauchy models. This resulted in two thicknesses for each EUV induced carbon sample: 2.7 and 5 nm for the sample exposed for 2 million pulses and 12–22.5 nm for the sample exposed to 5 million pulses. The small values correspond to the Cauchy model, while the large values result from the Tauc–Lorentz model. Ellipsometry was also used to determine that the background level of hydrocarbon adsorption for the masked part of the MLM was ~0.5 nm thick. The layer thicknesses that we quote are the difference in carbon layer thickness between the exposed and unexposed sections of the MLM. The masked sections of the MLMs exposed to graphitic carbon were found to be identical to an unexposed MLM, indicating that the carbon did not diffuse under the mask.

2.2. LG-SAW experimental equipment

Fig. 1 shows a diagram of the LG-SAW experimental setup. A SAW pulse was generated by a nitrogen pulsed laser, with a center wavelength of 337 nm, a pulse energy of 0.4 mJ and a pulse duration of 0.5 ns (FWHM). The laser beam was focused using a cylindrical lens to a stripe of approximately 8 by 0.012 mm, corresponding to an energy density of 417 mJ/cm^2, which is low enough to only excite the thermal expansion that generates a line-shaped broadband SAW pulse. An alignment bar was used to ensure that the SAW always propagated along the [110] direction of the (001) Si substrate. This is necessary due to the fact that the SAW velocity is not isotropic for the underling crystalline silicon substrate. The generated SAW pulses were detected by a piezoelectric transducer that was fixed on the mirror. More details on the experimental apparatus and following signal analysis can be found in reference [5].

The SAW pulses were detected at several different propagation distances, ranging from less than 1 cm to a few cm by translating the MLM sample with a high precision stage. The pulses were acquired by a digitizing oscilloscope, which was then transferred to a computer for computation. Amplitude and phase spectra of the pulse signals are calculated by taking the Fourier transform of a cross correlation between the piezoelectric detector's response at the shortest distance and with the responses at all other distances. The SAW dispersion curve is deduced from the phase spectra. The frequency range of the dispersion curve is determined by requiring that the amplitude of the frequency components be sufficient large.

The experimental dispersion curves were used to determine the mechanical properties of the MLM and the carbon film by fitting a theoretical dispersion curve to the measured curve by varying the related parameters, such as Young's modulus, density, Poisson ratio, and thickness. The number of parameters that can be independently

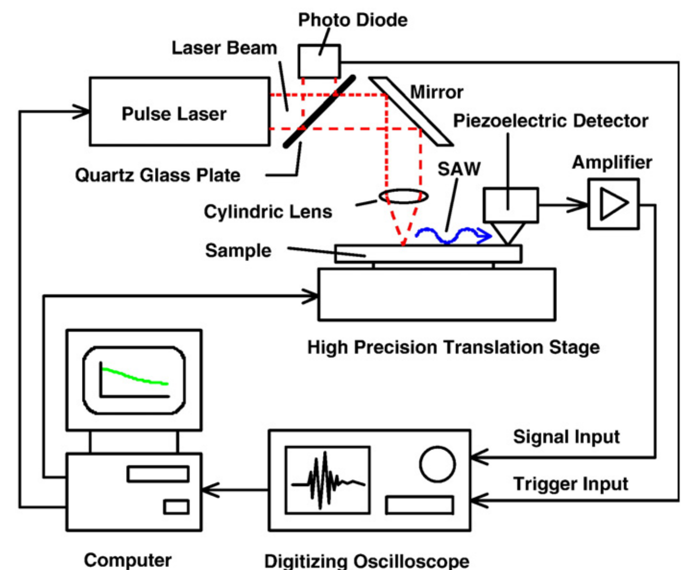

Fig. 1. The system diagram of LG-SAW experimental setup.

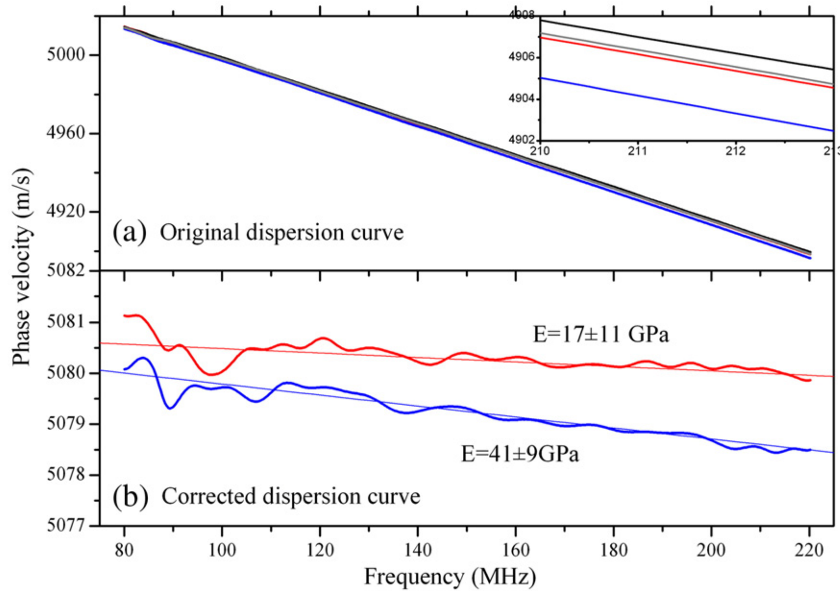

Fig. 2. Dispersion curves measured for MLM with EUV induced carbon deposited on them. The original dispersion curves obtained from the raw data (a) with an expanded section shown in the inset figure. The black and grey lines are the dispersion curves of the unexposed MLM, while the red line and blue lines correspond to a 5 and a 22.5 nm thick carbon layer respectively. Subfigure (b) shows the dispersion curves with the influence of the MLM removed (see text for details). The red and blue curves correspond to the measured (thick lines) and calculated (thin lines) dispersion of the 5 and 22.5 nm thick carbon layers respectively.

determined depends on the film thickness and the difference between the mechanical properties of the film and the substrate. Note that the degree of nonlinearity of the SAW dispersion curve is crucial for determining the number of parameters that can be independently resolved.

3. Results

LG-SAW measurements were performed on both the exposed and unexposed sections of the MLM samples. The dispersion curves obtained from the MLMs with EUV induced carbon and hot filament carbon are shown in Figs. 2(a) and 3(a). In general, SAW pulses with wide frequency bandwidth up to 220 MHz were generated and detected. All the dispersion curves are nearly linear and exhibit normal dispersion (i.e. velocity decrease for increasing frequency), thus we can only determine a single parameter—Young's modulus—with *a priori* knowledge of the film density, thickness, and Poisson's ratio. Extrapolating all the dispersion curves to zero frequency reveals the SAW velocity for the substrate to be about 5081 m/s, which agrees with the propagation velocity in the [110] direction on a clean (001) silicon wafer. This is expected since the thickness of the whole multilayer (357 nm) and carbon film is small compared to the penetration depth of the SAW spectrum which is roughly comparable to the respective SAW wavelength (ca. 20–60 μm). Taking into account the well defined layer thicknesses for the MLM, and using the average value of Poisson's ratios of Mo and Si, and average densities that are

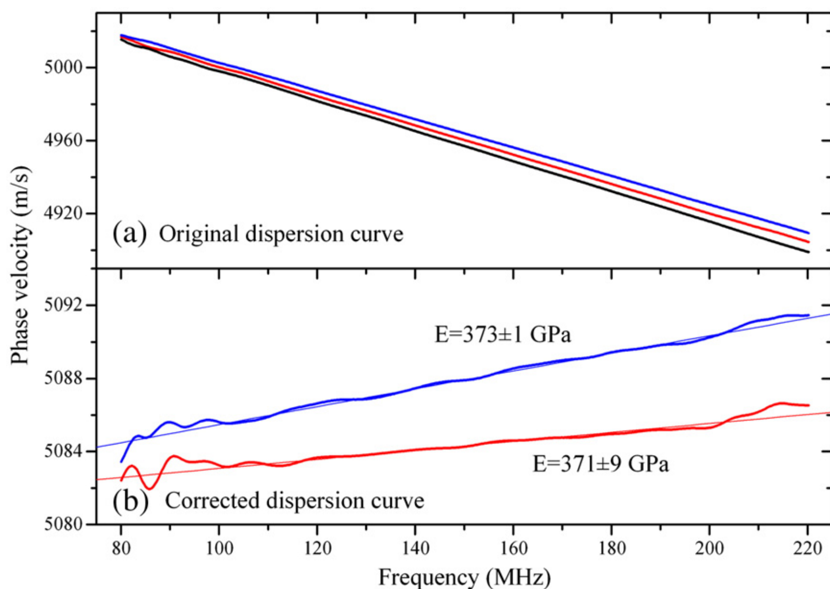

Fig. 3. Dispersion curves measured for MLM with hot filament carbon deposited on them. The original dispersion curves obtained from the raw data are shown in (a). The black line is the dispersion of an unexposed MLM, while the red line and blue lines correspond to an 11.9 and a 24.3 nm thick carbon layers respectively. Subfigure (b) shows the dispersion curves with the influence of the MLM removed (see text for details). The red and blue curves correspond to the measured (thick lines) and calculated (thin lines) dispersion of the 11.9 and 24.3 nm thick carbon layers respectively. (For interpretation of the references to colour in this figure legend, the reader is referred to the web version of this article.)

85% of the bulk value [12], we find that the effective Young's modulus for the MLM is 168 GPa, which is smaller than the average value of the Young's modulus for the bi-layer system.

We obtain the contribution of the EUV induced carbon layer by subtracting the dispersion due to the MLM from the total dispersion curve (see Fig. 2(b)). For each MLM, the dispersion from the unexposed section served as a reference. Subtraction implicitly assumes linearity, which is only valid when the layer thicknesses of the whole multilayer (357 nm) and the carbon layer (<25 nm) is small compared to the wavelength of the SAW (ca. 20–60 μm) and the corresponding SAW dispersion can be considered to be a small perturbation of the substrate dispersion [13]. The corrected curve, since it removes the dispersion of the MLM, is assumed to be the dispersion of the carbon layer as if it were directly deposited on the silicon wafer. The oscillation features at both limits of the frequency range are caused by the frequency characteristic and are not relevant to our analysis.

As can be seen in Fig. 2(b), the slope of the corrected dispersion curve is quite close to zero for both films, though still negative, indicating that the Young's modulus of EUV induced carbon is smaller than that of the Si wafer (169 GPa). Since the dispersion curve is linear, a value for Young's modulus can only be obtained if the density, Poisson's ratio, and layer thickness are known. Normal dispersion indicates that the film cannot be diamond-like because Young's modulus must be less than 169 GPa, thus, the layer thicknesses obtained from the Tauc–Lorentz model were used (5 and 22.5 nm). Hydrogenated amorphous carbon films have been observed to have a density in the range of 1.0–1.6 g/cm^3 [14]. However, we restrict the range of values to 1.2–1.6 g/cm^3 because the predicted values for Young's modulus at densities lower than 1.2 g/cm^3 are too low for a solid film. Poisson's ratio is relatively constant between different polymeric films with a value of 0.5.

Using these parameter ranges, Young's modulus was found to be 17 ± 11 and 41 ± 9 GPa for the 5 and the 22.5 nm thick films, respectively. The uncertainty in range for Young's modulus is obtained from the average and standard deviation for Young's moduli derived from multiple data sets obtained from the same location. This accurately reflects the contribution of the 0.1 m/s uncertainty in the velocity data in the original dispersion curve and also includes the influence of possible changes in the film density.

Young's modulus clearly increased with increasing thickness. It is typical to find that for films of a few nanometers thickness, the density increases as the film thickness increases until the bulk value is obtained. Thus, it is reasonable to expect that the density and Young's modulus of the thinner EUV induced carbon film is less than that of the thick layer. Alternatively, both layers may not yet be fully polymerized from the background, short chain hydrocarbons, resulting in a much more fluid-like surface with a very small Young's modulus but similar density.

A similar analysis was performed on MLMs that had hot filament carbon layers deposited on them. Fig. 3(a) shows the dispersion curves of the MLM and carbon layers. The corrected dispersion in Fig. 3(b) is also linear, but with a positive slope, clearly showing the anomalous dispersion of the carbon layer. This indicates that it has a Young's modulus larger than that of the underlying silicon substrate. Since deposition took place using a pure carbon source in background conditions with no detectable hydrogen, the layers are expected to be hydrogen free amorphous carbon. Consequently, we assume that Poisson's ratio is 0.19, as is typical for hydrogen free, amorphous carbon. The density and Young's modulus for carbon deposited in this manner have been observed to be related by an empirical relationship, which we use to eliminate the density as a free parameter in the fitting procedure [15].

By fitting the corrected dispersion curve it was obtained that the Young's modulus for hot filament carbon was 371 ± 9 GPa and 373 ± 1 GPa for the 11.9 nm for 24.3 nm thick films, respectively. These two values are in the general range of amorphous carbon films.

In contrast to the EUV induced carbon, the values for Young's modulus are consistent between the two film thicknesses, indicating that the carbon layer's density and morphology do not change much over the course of the deposition by this method. This is not unexpected since the deposition time is very short and the MLM surface temperature was kept at room temperature, leaving little chance for annealing. On the other hand, EUV induced carbon is subject to constant bombardment by ~90 eV photons and lower energy photoelectrons during a deposition process that lasts for 2–5 h.

4. Conclusions

We have presented the first LG-SAW experiments on MLM structures with a further layer of carbon deposited on top of that using two different deposition methods: hot filament deposited carbon and EUV photo-induced hydrocarbons. The mechanical properties of two different carbon films have been analyzed and compared. The Young's modulus of the hot filament carbon was about 370 GPa, which is in the general range of amorphous carbon films. Furthermore, the consistency of the measurements indicates that the carbon layer's mechanical properties do not change significantly as the layer thickness increases. However, carbon layers deposited from ambient hydrocarbons under illumination of EUV radiation had a Young's modulus that increased significantly with layer thickness. The small Young's modulus (<100 GPa) leads us to conclude that EUV induced carbon is mechanically soft, and polymer-like. In addition, it was also found that LG-SAW is sensitive enough to detect EUV induced carbon growth less than 5 nm, which is within an order of magnitude of the sensitivity required for EUVL contamination monitoring.

Acknowledgements

This research was carried out under the project number MC3.06245 in the framework of the Research Program of the Materials Innovation Institute M2i (www.m2i.nl), the former Netherlands Institute for Metals Research, the “Stichting voor Fundamenteel Onderzoek der Materie FOM,” the latter being financially supported by the “Nederlandse Organisatie voor Wetenschappelijk Onderzoek NWO” and Senter-Novem through the “ACHieVE” programme. We gratefully acknowledge Herbert Wormeester at University of Twente for ellipsometry experiments.

References

[1] S. Oestreich, R. Klein, F. Scholze, J. Jonkers, E. Louis, A.E. Yakshin, P.C. Goerts, G. Ulm, M. Haidl, F. Bijkerk, Soft X-Ray and EUV Imaging Systems, SPIE, San Diego, CA, USA, 2000, p. 64.
[2] G. Kyriakou, D.J. Davis, R.B. Grant, D.J. Watson, A. Keen, M.S. Tikhov, R.M. Lambert, Journal of Physical Chemistry C 111 (2007) 4491.
[3] S. Matsunari, T. Aoki, K. Murakami, Y. Gomei, S. Terashima, H. Takase, M. Tanabe, Y. Watanabe, Y. Kakutani, M. Niibe, Y. Fukuda, Emerging Lithographic Technologies XI, SPIE, San Jose, CA, USA, 2007, p. 65172X.
[4] B. Johs, J.A. Woollam, C.M. Herzinger, J. Hilfiker, R. Synowicki, C.L. Bungay, SPIE, SPIE, Denver, Colorado, 1999, p. 29.
[5] D. Schneider, T. Schwarz, Surface & Coatings Technology 91 (1997) 136.
[6] D. Schneider, B. Schultrich, Surface & Coatings Technology 98 (1998) 962.
[7] M. Weihnacht, K. Franke, K. Kammer, R. Kunze, H. Schmidt, IEEE Ultrasonics Symposium, 1997, p. 217.
[8] E. Louis, H.J. Voorma, N.B. Koster, L. Shmaenok, F. Bijkerk, R. Schlatmann, J. Verhoeven, Y.Y. Platonov, G.E. Vandorssen, H.A. Padmore, Microelectronic Engineering 23 (1994) 215.
[9] K. Bergmann, O. Rosier, R. Lebert, W. Neff, R. Poprawe, Microelectronic Engineering 57–8 (2001) 71.
[10] C. Tanguy, Physical Review B 60 (1999) 10660.
[11] G.E. Jellison, F.A. Modine, Applied Physics Letters 69 (1996) 2137.
[12] H.J. Voorma, E. Louis, N.B. Koster, F. Bijkerk, E. Spiller, Journal of Applied Physics 81 (1997) 6112.
[13] D. Schneider, T. Witke, T. Schwarz, B. Schoneich, B. Schultrich, Surface & Coatings Technology 126 (2000) 136.
[14] J. Robertson, Materials Science & Engineering. R, Reports 37 (2002) 129.
[15] D. Schneider, T. Schwarz, H.J. Scheibe, M. Panzner, Thin Solid Films 295 (1997) 107.